Durham University

Durham Research Online

Deposited in DRO:

30 August 2016

Version of attached file:

Accepted Version

Peer-review status of attached file:

Peer-reviewed

Citation for published item:

Desseaux, S. and Hinestrosa, J. P. and Schüwer, N. and Lokitz, B. and Ankner, J. F. and Kilbey II, S. M. and Voïtchovsky, K. and Klok, H.-A. (2016) 'Swelling behavior and nanomechanical properties of (peptide-modified) poly(2-hydroxyethyl methacrylate) and poly(poly(ethylene glycol) methacrylate) brushes.', Macromolecules., 49 (12). pp. 4609-4618.

Further information on publisher's website:

http://dx.doi.org/10.1021/acs.macromol.6b00881

Publisher's copyright statement:

This document is the Accepted Manuscript version of a Published Work that appeared in final form in Macromolecules, copyright © American Chemical Society after peer review and technical editing by the publisher. To access the final edited and published work see http://dx.doi.org/10.1021/acs.macromol.6b00881

Additional information:

Use policy

The full-text may be used and/or reproduced, and given to third parties in any format or medium, without prior permission or charge, for personal research or study, educational, or not-for-profit purposes provided that:

- a full bibliographic reference is made to the original source
- a link is made to the metadata record in DRO
- the full-text is not changed in any way

The full-text must not be sold in any format or medium without the formal permission of the copyright holders.

Please consult the full DRO policy for further details.

Durham University Library, Stockton Road, Durham DH1 3LY, United Kingdom
Tel : +44 (0)191 334 3042 | Fax : +44 (0)191 334 2971
http://dro.dur.ac.uk

Swelling Behavior and Nanomechanical Properties of (Peptide-modified) Poly(2-Hydroxyethyl Methacrylate) and Poly(Poly(Ethylene Glycol) Methacrylate) Brushes

Solenne Desseaux,[1,a] Juan Pablo Hinestrosa,[1,a] Nicolas Schüwer,[1] Bradley S. Lokitz,[2] John F. Ankner,[3] S. Michael Kilbey, II,[4] Kislon Voitchovsky,[5] Harm-Anton Klok[1]*

1. École Polytechnique Fédérale de Lausanne (EPFL), Institut des Matériaux et Institut des Sciences et Ingénierie Chimiques, Laboratoire des Polymères, Bâtiment MXD, Station 12, CH-1015 Lausanne, Switzerland.

2. Center for Nanophase Material Sciences, Oak Ridge National Laboratory, One Bethel Valley Road, Oak Ridge, Tennessee 37831, United States.

3. Spallation Neutron Source, Oak Ridge National Laboratory, Oak Ridge, Tennessee 37831, United States.

4. Departments of Chemistry and Chemical & Biomolecular Engineering, University of Tennessee, Knoxville TN 37996-1600, United States.

5. Durham University, Department of Physics, South Road, Durham DH1 3LE, UK.

[a] these authors contributed equally to this study.

solenne.desseaux@empa.ch, hinestrosajp@gmail.com, nicolas_schuewer@nittoeur.com, lokitzbs@ornl.gov, anknerjf@ornl.gov, mkilbey@utk.edu, kislon.voitchovsky@durham.ac.uk, harm-anton.klok@epfl.ch

* Corresponding author. Email: harm-anton.klok@epfl.ch; Fax: + 41 21 693 5650; Tel.: + 41 21 693 4866.

ABSTRACT

Poly(2-hydroxyethyl methacrylate) (PHEMA) and poly(poly(ethylene glycol) methacrylate) (PPEGMA) brushes represent a class of thin, surface-tethered polymer films that have been extensively used e.g. to generate non-biofouling surfaces or as model systems to study fundamental biointerfacial questions related to cell-surface interactions. As the properties of PHEMA and PPEGMA brushes depend on the hydration and swelling of these thin films, it is important to understand the influence of basic structural parameters such as the composition of the polymer brush, the film thickness or grafting density on these phenomena. This manuscript reports results of a series of experiments that were performed to investigate the swelling behavior and mechanical properties of a diverse library of PHEMA and PPEGMA brushes covering a range of film thicknesses and grafting densities. The swelling ratios of the PHEMA and PPEGMA brushes were determined by ellipsometry and neutron reflectivity experiments and ranged from ~ 1.5 - ~ 5.0. Decreasing the grafting density and decreasing the film thickness generally results in an increase in the swelling ratio. Modification of the PHEMA and PPEGMA brushes with the cell adhesion RGD peptide ligand was found to result in a decrease in the swelling ratio. The neutron reflectivity experiments further revealed that solvated PHEMA and PPEGMA brushes are best described by a two-layer model, consisting of a polymer-rich layer close to the substrate and a second layer that is swollen to a much higher degree at the brush – water interface.

INTRODUCTION

The interactions between synthetic and biological materials are governed by a complex interplay of biochemical cues (typically proteins or peptides presented at the synthetic materials surface) as well as the topography[1] and mechanical properties[2] of the synthetic surface/interface. Deciphering and understanding the contributions of each of these factors is a challenging but important task[3] that is required to efficiently design novel biomaterials that can be tuned to guide cell adhesion, proliferation and differentiation, which are important processes inherent to areas such as tissue repair and regeneration.[4]

To obtain insight into and answer these fundamental biointerfacial questions, there is an interest in model systems that allow to independently investigate the influence of surface biochemistry, topography and mechanical properties on cell behavior. One class of model biointerfaces that has attracted a lot of interest are thin polymer films generated by surface-initiated controlled radical polymerization.[5,6] These thin films, which consist of densely grafted assemblies of chain-end tethered polymers are also colloquially referred to as "polymer brushes". There are a number of reasons that make polymer brushes attractive model systems to investigate the interactions between synthetic, soft materials and biological systems. First of all, the thickness (d), grafting density (σ) and chemical composition of these thin films can be accurately controlled using any of the well-established surface-initiated (controlled) polymerization techniques. Furthermore, surface-initiated (controlled) radical polymerization techniques are compatible with many micropatterning tools, which allows facile access to e.g. microstructured substrates, and also can be used to conformally coat complex, 3D structured substrates.[7] Polymer brush based model biointerfaces are generally obtained by surface-initiated polymerization of hydrophilic, water-soluble monomers, which results in thin, hydrogel-like films that resist non-specific adhesion of proteins and cells.[8] The ability to resist non-specific adhesion of proteins and cells is important because it allows these

polymer brushes to be used as platforms to screen and understand the influence of surface biochemistry on cell behavior.[6] While a variety of monomers has been used to generate polymer brush based model biointerfaces (including e.g. methacrylic acid[9,10,11] and zwitterionic monomers[12]), 2-hydroxyethyl methacrylate (HEMA) and poly(ethylene glycol) methacrylate (PEGMA) are particularly frequently employed as they allow access to polymer brush films that possess very efficient non-fouling properties and present side-chain functional hydroxyl groups, which provide a wide range of possibilities to introduce biochemical cues.[13,14,15,16]

PHEMA and PPEGMA brushes will swell in aqueous media, which has important conseqences on the properties of these thin films. On the one hand, hydration, and, as a consequence, swelling, of these surface grafted polymer films is an important contributor to their ability to resist non-specific adhesion of proteins and cells. Hydration and swelling, however, will also impact the modulus, or more generally, the mechanical properties of the films. As it is known that cells respond to the stiffness of their substrates,[2] this may influence adhesion, spreading and proliferation of cells on PHEMA and PPEGMA brushes modified with appropriate peptide ligands. The swelling of water-swellable brushes, including PHEMA and PPEGMA brushes is governed by a complex interplay of several variables, including film thickness, grafting density as well as the chemical composition of the brush and that of the aqueous medium (most importantly pH and ion strength).[17,18] Investigating and understanding the contributions of each of these parameters is a challenging task, yet would provide useful insight for the design of polymer brush films with predictable properties.

Some work has been done to investigate the swelling behavior and mechanical properties of PHEMA and PPEGMA brushes. Swollen polymer brushes are often characterized in terms of their swelling ratio, which is the ratio of the swollen film thickness to the thickness in the dry state. Tranchida et al., for example, have used atomic force microscopy (AFM) cross-

sectional analysis to study the swelling properties of densely grafted (i.e. brushes grafted from surfaces uniformly modified with a tethered initiator) poly(diethylene glycol methyl ether methacrylate) (PDEGMA) brushes with a dry film thickness of 41 nm and found a swelling ratio of ~ 1.8.[19] These authors also investigated mechanical properties using AFM nanoindentation experiments and reported elastic moduli of 764 kPa and 3240 kPa for water-swollen PDEGMA and poly((oligo ethylene glycol) methacrylate) brushes with dry film thicknesses of 40 nm.[19] A library of 3 poly((ethylene glycol) methyl ether methacrylate) brush samples was studied by Brash and coworkers using neutron reflectivity. These samples had dry film thicknesses and grafting densities of 281 Å/0.39 chains×nm^{-2}, 88 Å/0.39 chains×nm^{-2} and 52 Å/0.07 chains×nm^{-2} and swelling ratios of 1.5, 1.6, and 4.1, respectively.[20] Fu et al. used ellipsometry to evaluate the swelling of densely-grafted poly((oligo ethylene glycol) methacrylate) brushes that had dry films thicknesses between 25 and 35 nm and found a swelling ratio around 2.[21] Bao et al. studied the swelling behavior of PHEMA brushes grown from gold substrates modified with mixed monolayers of an ATRP active and a dummy thiol. Using ellipsometry, it was found that brushes grafted from substrates that presented 5, 50 or 100 % of the ATRP active thiol showed swelling ratios of ~ 1.6 – 1.8, whereas for brushes that were prepared from surfaces that presented 0.1 % or 1 % of the ATRP active thiol swelling ratios of 18, respectively 2.6 were determined.[22] These authors also noted that the swelling behavior of PHEMA brushes is very likely to be influenced by the lightly crosslinked nature of these films as well.

While the examples discussed above do provide useful insight into the effects of film thickness and grafting density of PHEMA and PPEGMA brushes on their swelling behavior and mechanical properties, there is a vast parameter space, the effects of which remain unexplored. This includes amongst others, studying libraries of samples that cover a broader range of film thicknesses and grafting densities in order to establish robust structure-property

relationships. Another important aspect would be to systematically study the influence of the chemical composition of the polymer brush films on swelling behavior and mechanical properties across a series of samples of (nearly) identical grafting densities and polymer molecular weight. For PHEMA and PPEGMA based brushes, this could also entail investigating the effect of the number of ethylene glycol units in the side chains of these polymers. A final important question relates to the influence of cell-adhesive peptide ligands on the properties of PHEMA and PPEGMA based polymer brush films. This manuscript reports results from a number of experiments that aim to address some of these challenges using a diverse library of PHEMA and PPEGMA brush samples that cover a relatively wide range of film thicknesses and grafting densities. Some of the samples were further functionalized with the cell adhesive RGD peptide ligand.[23] The swelling behavior of the (peptide-functionalized) polymer brushes has been investigated with ellipsometry, neutron reflectivity as well as atomic force microscopy (AFM) experiments whereas the nanomechanical properties of these films were evaluated with AFM. The collective results of these experiments not only shed light on the effects of film thickness and grafting density on the swelling behavior and mechanical properties of oligo(ethylene glycol) side chain functional polymethacrylate brushes, but also provide insight into the effects of the chemical composition of the brush (more specifically: the number of ethylene glycol units in the side chain functional groups) as well as the presence of cell adhesive peptide ligands.

EXPERIMENTAL SECTION

Materials. 2-Hydroxyethyl methacrylate (HEMA, 97 %), poly(ethylene glycol) methacrylate ($M_n \approx 360$ g.mol^{-1}, $PEGMA_6$), poly(ethylene glycol) methacrylate ($M_n \approx 500$ g.mol^{-1}, $PEGMA_{10}$) (the subscripts in $PEGMA_6$ and $PEGMA_{10}$ indicate the number of ethylene glycol side chain repeat units), copper (I) chloride (99.99 %), copper (II) bromide (99.999 %), 2,2-

bipyridyl (bipy, 99 %), 4-nitrophenylchloroformate (NPC, 96 %), 4-(dimethylamino)pyridine (DMAP, 99 %) and methanol were purchased from Sigma Aldrich and used as received unless specified otherwise. The GGGRGDS peptide (purity > 98 %) was obtained from GLBiochem (Shanghai, China). The ATRP initiator (6-(2-bromo-2-methyl)propionyloxy)hexyldimethylchlorosilane (**1**) and its inactive equivalent (**2**) were synthesized as previously reported.[24,25] The inhibitor was removed from HEMA, $PEGMA_6$ and $PEGMA_{10}$ by passing the monomers through a column of basic alumina. Water was obtained from a Millipore Milli-Q gradient machine equipped with a 0.22 μm filter. Toluene was purified and dried using a solvent-purification system (PureSolv). PBS concentration was 0.01 M with a pH of 7.4. For neutron reflectometry studies, brushes were grown from 2 inch diameter, 5 mm thickness silicon wafers that were obtained from El-Cat, Inc. For all other experiments, silicon substrates ((100) orientation) of size 8 mm x 10 mm were used to grow polymer brushes.

Methods.

XPS. X-ray photoelectron spectroscopy (XPS) was carried out using an Axis Ultra instrument from Kratos Analytical equipped with a conventional hemispheric analyzer. The X-ray source employed was a monochromatic Al Kα (1486.6 eV) source operated at 100 W and 10^{-9} mbar.

Spectroscopic Ellipsometry. Dry brush thicknesses and refractive index profiles were determined using a J. A. Woollam M-2000U variable angle spectroscopic ellipsometer over a wavelength range (λ) of 250 to 800 nm. To fit the ellipsometric data, each polymer brush was modeled as a slab of uniform optical properties and a two parameter Cauchy model $n(\lambda) = A + B/\lambda^2$ was used to characterize the refractive index as a function of wavelength (Figure S1). The values of A and B reported in Table S1 in the Supporting Information represent the

average of three different brush samples for each type of monomer at a grafting density of σ = 100 %.

Phase Modulated Ellipsometry. A Beaglehole Picometer ellipsometer, which uses a HeNe laser (λ = 632.8 nm), was used to determine the thickness of brushes swollen in water. Brush-modified silicon surfaces were mounted and aligned in the center of a custom-made cylindrical fluid cell made of optical quality glass,[17] and the ellipticity, ϱ , expressed in terms of the real and imaginary components Re (ϱ) and Im (ϱ), was measured at angles of incidence ranging from 80° to 50° in increments of 1°. From these values, simultaneous fitting of the swollen thickness (d_{wet}) and swollen brush refractive index (n_b) is performed using the built-in software. From the n_b values it is possible to estimate the fraction of polymer in the swollen brush (ϕ) using the Bruggeman effective medium approximation.[26]

$$\varphi \frac{n_P^2 - n_b^2}{n_P^2 + 2n_b^2} + (1-\varphi)\frac{n_S^2 - n_b^2}{n_S^2 + 2n_b^2} = 0 \quad (1)$$

Here n_P is the refractive index of the polymer brush in "dry" conditions as measured by spectroscopic ellipsometry (at λ = 632.8 nm, see Table S1) and n_S is the refractive index of solvent water, n_S = 1.333. It is useful to remember that analyses of ellipsometric data treats the (solvated) brush layer as a "slab" of uniform density and models the brush/solution interface as infinitely sharp.

Neutron reflectivity (NR). Measurements were performed using the Liquids Reflectometer (NR) of the Spallation Neutron Source at Oak Ridge National Laboratory. This instrument collects specular reflectivity in continuous wavelength bands at several incident angles to span a total wave vector transfer (q) from 0.006 $Å^{-1}$ to 0.17 $Å^{-1}$. Data were collected in a manner such that the relative resolution, dq/q, was constant at 0.05, which allows the specular reflectivity collected at different wavelength bands and incident angles to be "stitched together" into a single reflectivity curve. The reflectivity measured for dry brushes was fit using a three layer model consisting of "slabs" that represent the silicon substrate (Si), the

silicon oxide layer (SiO_x) and the polymer brush, with air as the incident media. Each slab is represented by its thickness, interfacial roughness and scattering length density (Σ). Of these, only the Σ of the polymer film, its thickness and the interfacial roughnesses that characterize the Si/SiO_x, SiO_x/polymer and polymer/air interfaces are adjusted when fitting the data. The Σ values for each monomer (Σ_m) were calculated from elemental contributions with the density of the brushes assumed to be 1.2 g/cm^3 thus yielding; HEMA ($C_6H_{10}O_3$): 1.10×10^{-6} Å^{-2}; $PEGMA_6$ ($C_{16}H_{30}O_8$): 8.37×10^{-7} Å^{-2}; $PEGMA_{10}$ ($C_{24}H_{40}O_{12}$): 7.84×10^{-7} Å^{-2}.[27] Reflectivity calculated using the Parratt formalism was compared to the measured reflectivity and optimized for goodness-of-fit.

NR measurements of the swollen brushes in D_2O were performed in a custom made fluid cell. Swelling of the brush increases the layer thickness and changes the interfacial roughness (transition region from brush to solvent), and as water penetrates into the brush, the scattering length density of the interfacial layer also changes. To handle this situation, mass balance is invoked to constrain the fitting of the solvated brushes:

$$d_{dry} = \sum_{i=1}^{i=n} \left(d_{wet}\varphi\right)_i \tag{2}$$

In essence, this mass balance constraint ensures that the total amount of polymer is held constant between the dry and swollen states. With this in mind, and because neutrons "see" nuclei per unit volume, the scattering length density of the swollen brush, Σ_i, is simply expressed as the volume fraction weighted sum of the scattering length densities of polymer, Σ_m, and D_2O, Σ_{D2O}, where ϕ is the volume fraction of polymer in the swollen brush:

$$\Sigma_i = \varphi\Sigma_m + (1-\varphi)\Sigma_{D_2O} \tag{3}$$

The value of $\Sigma_{D2O} = 6.34 \times 10^{-6}$ Å^{-2}. The combination of these two elements – preserving mass balance between dry and solvated brushes, and using the amount (volume fraction) of water entering the brush to govern the total swelling of the brush – significantly constrain the

fitting by limiting the number of adjustable parameters. Perhaps more importantly, these constraints help to develop a credible physical representation of the solvated brush system.[18,28] As before, fits of wet brushes again are optimized for goodness-of-fit (χ^2).

Water Contact Angle (WCA) measurements. Static water contact angles were measured at ambient conditions using a DataPhysics OCA 35 contact angle measuring instrument.

Atomic Force Microscopy. AFM measurements were performed on a commercial Bruker Multimode Nanoscope IIIa instrument (Bruker, Santa Barbara, CA) equipped with a liquid cell. The cantilever spring constants (Olympus RC800PSA) were determined using their thermal spectra.[29] *Film thickness and roughness measurements*. Tapping mode was used to obtain topography images. Layer thicknesses were determined from cross-sectional height profiles of micropatterned polymer brushes, which were prepared on silicon substrates following an established protocol.[30] The measurements were carried out in air, Milli-Q water and/or PBS. The roughness was obtained from the topography images (scan size 2 x 2 μm^2). *Apparent Young's moduli*. The Young's Moduli of unmodified and RGD-modified brushes immersed in PBS solution were calculated from indentation curves. In order to improve the reliability of the results, indentation curves were acquired systematically over different locations of the sample (256 curves, evenly distributed over 2 μm^2). The curves were analyzed following procedures described elsewhere[31] using custom-made routines programmed in the Igor Pro software environment (Lake Oswego, OR, USA).[31] As an example, Figure S2 (Supporting Information) shows a set of indentation curves recorded on a RGD-modified PHEMA brush. To determine the apparent Young's Modulus of the solvated brush, the indentation curves were fit with the Hertz model[31] $F = \frac{4\sqrt{R}}{3(1-\upsilon^2)} E\delta^{3/2}$ where R is the contact radius (approximated as the tip radius), υ is Poisson's ratio (taken as ½ assuming incompressibility), δ the indentation depth and E is the apparent Young Modulus. For the

fitting procedure, the tip radius provided by the manufacturer was used. We note that the Hertz model does not take into account the finite thickness of the brush and the influence of the stiff substrate underneath, and may hence overestimate the resulting moduli. However, the limited depth of indentation (compared to the brush's thickness) should limit this effect. An additional source of error is the approximation of a constant contact radius equal to that of the tip. The associated error, however, is small compared to other sources considering the dependence on √R. Here these errors are mitigated by the systematic approach and the fact that we place the emphasis on the relative differences in stiffness between samples rather than the absolute values. To ensure reliability of the results, a full set of data was acquired in three different locations of each sample. All the results for a given sample were combined in a histogram, which was subsequently fitted with a Gaussian curve in order to derive an average modulus and its uncertainty. An example of such a histogram for an RGD post-functionalized PHEMA brush with an initial dry film thickness of 52 nm is shown in Figure S3.

Preparation of polymer brushes.

ATRP-initiator modified substrates. ATRP initiator-modified substrates were prepared following a previously published protocol using appropriate mixtures of the ATRP active (**1**) and ATRP inactive chlorosilane (**2**).[25] The grafting densities (σ) that are reported throughout this paper are expressed as volume % of the ATRP active chlorosilane.

Surface-Initiated ATRP of HEMA. PHEMA brushes were grown following a literature procedure with CuCl/$CuBr_2$/bipy as the catalyst system.[14]

Surface-Initiated ATRP of $PEGMA_6$. For the NR and ellipsometry experiments, $PPEGMA_6$ brushes were grown following a literature procedure with CuCl/$CuBr_2$/bipy as the catalyst system.[14] For the AFM experiments, $PPEGMA_6$ brushes were grown following a literature procedure with CuCl/bipy as the catalyst system.[32]

Surface-Initiated ATRP of $PEGMA_{10}$. For the NR and ellipsometry experiments, $PPEGMA_{10}$ brushes were grown following a literature procedure with $CuCl/CuBr_2$/bipy as the catalyst system and for the AFM experiments, $PPEGMA_{10}$ brushes were grown following a literature procedure with $CuBr/CuBr_2$/bipy as the catalyst system.[14]

Peptide functionalization. Post-polymerization modification of the side-chain hydroxyl groups of the PHEMA and PPEGMA brushes with the GGGRGDS peptide was performed according to a published protocol.[14,33]

RESULTS AND DISCUSSION

Polymer Brush Synthesis and Characterization. Scheme 1 outlines the synthesis of the polymer brushes investigated in this manuscript. The samples studied here were prepared by surface-initiated atom transfer radical polymerization (SI-ATRP) of 2-hydroxyethyl methacrylate (HEMA) as well as two poly(ethylene glycol) methacrylate monomers that differ with respect to the average number of side-chain ethylene glycol repeats, viz. $PEGMA_6$ and $PEGMA_{10}$. These monomers were selected as they are widely used for the fabrication of model biointerfaces and combine excellent non-fouling properties with the presence of side-chain hydroxyl groups, which can be used to introduce biochemical cues via post-polymerization modification.[34] Polymer brushes covering a range of film thicknesses and grafting densities (σ) were obtained by adjusting the polymerization time and the volume percentage of the ATRP initiator modified chlorosilane (**1**) that was used to modify the substrates. SI-ATRP of HEMA and PEGMA is known to result in lightly crosslinked polymer brushes.[22,35] The crosslinked nature of the brushes hampers cleavage and GPC analysis, which could enable to obtain information on the molecular weight of the surface grafted polymer chains and the grafting density of the polymer brush films. As a precise determination of the molecular weight and grafting density is not possible, the remainder of this manuscript will

use reaction time as a measure for the molecular weight of the surface grafted polymers and grafting densities will be expressed as a percentage, which indicates the volume % of the ATRP active organosilane **1** that was used to modify the silicon substrate (σ = 50, 75 and 100 %). RGD-functionalized polymer brushes were prepared by nitrophenylchloroformate (NPC) mediated post-polymerization modification of PHEMA, $PPEGMA_6$ and $PPEGMA_{10}$ brushes with σ = 100 % and different film thicknesses following an established protocol.[14] The peptide post-polymerization modification reactions were carried out using a 1 mM DMF solution of the GGGRGDS peptide, which typically results in peptide surface concentrations of 28 pmol/cm^2, 19 pmol/cm^2 and 14 pmol/cm^2 for PHEMA, $PPEGMA_6$ and $PPEGMA_{10}$ brushes, respectively.[14]

INSERT SCHEME 1

Figure 1 shows the evolution of the dry ellipsometric film thickness of PHEMA, $PPEGMA_6$ and $PPEGMA_{10}$ brushes as a function of polymerization time at grafting densities σ = 50 %, 75 % and 100 %. The corresponding 2D plots that present film thickness versus polymerization time for the different monomers and grafting densities together with the respective error bars are presented in Supporting Information Figure S4. For all three groups of polymer brushes, the dry film thickness, at a given grafting density, increases with increasing polymerization time, which is typical for surface-initiated controlled polymerization reactions and allows to prepare polymer brushes with defined film thicknesses by adjusting the polymerization time. While at any given polymerization time, the dry film thicknesses of the PHEMA brushes increase with increasing grafting density, the $PPEGMA_6$ and $PPEGMA_{10}$ film thicknesses are much less dependent on the grafting density.

INSERT FIGURE 1

All the polymer brush films were characterized by XPS, water contact angle analysis as well as atomic force microscopy (AFM). Figure 2 presents survey as well as C_{1s} and N_{1s} high resolution scans of a PHEMA brush (d = 52 nm; σ = 100 %) before and after post-polymerization modification with the GGGRGDS peptide (the corresponding XPS spectra for the $PPEGMA_6$ and $PPEGMA_{10}$ brushes are included in the Supporting Information, Figure S5 and Figure S6). The presence of an N_{1s} signal in the spectrum of the peptide-modified brush reflects the successful incorporation of the peptide. Table 1 reports the water contact angles of different polymer brush films (σ = 100 %) before and after peptide post-polymerization modification. The unmodified polymer brushes revealed very similar water contact angles, indicative of a hydrophilic surface. All contact angles measured were below 60°, which has been reported to be the threshold value for protein adhesion.[36] Post-polymerization modification with the GGGRGDS peptide did not result in significant changes in the water contact angle. The results listed in Table 1 also indicate that the film thickness of the different polymer brushes increases significantly upon post-polymerization modification with the GGGRGDS peptide. The increase in film thickness upon peptide modification, however, becomes less prominent as the number of ethylene glycol repeat units in the side chains of the monomer increases from 1 (PHEMA) to 10 ($PPEGMA_{10}$). This effect is due to the fact that the surface-concentration of side-chain hydroxyl groups in a $PPEGMA_{10}$ film is roughly half of that in a PHEMA brush.[14] Figure 3 presents 2 μm x 2 μm topography scans of dry films of the samples that are listed in Table 1. From cross-sectional analysis of these scans, the root mean square (RMS) dry film roughness of the different samples was estimated. For all samples, the RMS roughness was less than 1.2 nm (see Table 1), indicating that the SI-ATRP protocol used generates uniform and relatively smooth polymer films. Figure S7 in the

Supporting Information presents AFM topography scans and cross-sectional profiles of PBS-swollen, RGD-modified PHEMA, $PPEGMA_6$ and $PPEGMA_{10}$ brushes. Also swollen in PBS, these polymer brush films represent relatively smooth and uniform surfaces.

INSERT FIGURE 2

INSERT TABLE 1

INSERT FIGURE 3

Swelling and Nanomechanical Properties. Figure 4 summarizes the swelling ratios and polymer volume fractions (ϕ) as determined by ellipsometry for the three different classes of polymer brushes upon exposure to water. The swelling ratios are similar for all the polymers with most of the values between 1.5 and 3.5, which are comparable to values reported for other hydrophilic polymer brushes.[19,21,22,37] For samples with lower grafting density and smaller film thicknesses (i.e. shorter ATRP reaction times), the swelling ratios were found to increase to ~ 5. The swelling ratio decreases as polymerization time increases, suggesting that shorter chains have the tendency to be in a more relaxed state, i.e. mushroom regime, while longer chains are already more stretched in dry conditions due to steric hindrance. In agreement with earlier reported observations on e.g. poly(2-(dimethylamino)ethyl methacrylate)[17,37] and PNIPAm[38] brushes, the swelling ratios were also found to decrease with increasing grafting density. The grafting density dependence of the swelling ratio decreases from PHEMA to $PPEGMA_6$ to $PPEGMA_{10}$. The swelling ratios of the high grafting density brushes (σ = 100 %), which are reported in Table 1 and obtained by AFM are in good agreement with the ellipsometric data in Figure 4. As indicated by the data in Table 1, introduction of the RGD peptide in the PHEMA and PPEGMA brushes is accompanied by a decrease in the swelling ratio. This is attributed to the additional steric bulk of the GGGRGDS

peptide, which already leads to increased chain stretching (as compared to the unmodified brush) in the dry state and concomitantly to a reduced swelling upon exposure to aqueous media. Figure 4 also illustrates the changes in the polymer volume fraction in the swollen polymer brushes, as obtained from ellipsometry, as a function of polymerization time. The results for the three different brushes are qualitatively comparable and reveal an increase in the polymer volume fraction from 0.2 – 0.3 at short polymerization times to ~ 0.7 at longer polymerization times. Generally, the polymer volume fraction was found to increase with increasing grafting density.

INSERT FIGURE 4

Figure 5 shows the neutron reflectivity profiles for a PHEMA brush both in the dry and D_2O swollen state at σ = 100 %. The corresponding profiles for $PPEGMA_6$ and $PPEGMA_{10}$ brushes (σ = 100 %) are included in the Supporting Information (Figure S8 and S9). Table 2 and Figure 6 show the results from fitting the experimental data. While the data from the dry films could be fitted assuming a single polymer layer, the D_2O swollen films required a two-layer model featuring a significant amount of intermixing between the first and second polymer layers, but exhibiting a relatively smooth interface with the water subphase. The experimentally determined scattering length density values of the "dry" PHEMA, $PPEGMA_6$ and $PPEGMA_{10}$ brushes are 9.9×10^{-7} Å^{-2}, 7.7×10^{-7} Å^{-2}, 7.3×10^{-7} Å^{-2} , respectively, and slightly smaller than the predicted values (see Experimental Part). This difference may be ascribed to a difference between the nominal density and the actual (grafting) density as well as some hydration of the brush films in the "dry" state. The overall swelling ratio and the polymer volume fractions that can be derived from the neutron reflectivity experiments are in good agreement with the ellipsometry results. The roughnesses of the brush films as estimated

from neutron reflectivity are relatively small and range from 4.0 to 6.1 nm for the "dry" samples and from 7.9 – 13.2 nm for the D_2O swollen films. These numbers appear to be slightly larger compared to those reported in Table 1, but this is expected based on how the two different data analysis packages describe roughness.[18] The polymer density profiles of the swollen brushes that are shown in Figure 6 reveal that these thin films consist of a polymer-rich layer (ϕ = 0.85 - 0.90) close to the substrate and a second layer that is swollen to a much higher degree (ϕ = 0.50) at the brush – D_2O interface. This is an interesting observation as it indicates that these hydrophilic polymer brush films near the polymer – substrate interface only swell very little and are composed mostly of polymer.

INSERT FIGURE 5

INSERT FIGURE 6

INSERT TABLE 2

Apparent Young's moduli of the different polymer brushes in PBS both before as well as after post-polymerization modification with the RGD peptide were determined by AFM (Figure 7). For the interpretation of the results in Figure 7, it is important to keep in mind that SI-ATRP of HEMA, $PEGMA_6$ and $PEGMA_{10}$ generates lightly crosslinked polymer brush films. Another point worth noting is that RGD post-polymerization modification of the PHEMA and PPEGMA brushes does not necessarily result in a uniform distribution of the peptide ligands throughout the polymer brush film. The distribution and localization of the peptide ligands can also be probed using neutron reflectivity experiments.[25] As an example, the results of neutron reflectivity experiments on a PHEMA brush in the dry state before and after modification with the RGD peptide are included in Supporting Information Figure S10. The scattering length density profiles of the RGD modified PHEMA brush clearly indicate

that under the reaction conditions used in this study, the peptide ligands are preferentially located at the polymer brush – air interface.

The results in Figure 7 show that for the unmodified brushes Young's moduli of 1 - 4 MPa were obtained, except for the thickest $PPEGMA_{10}$ brush, which had an apparent Young's modulus of 14 MPa. The moduli measured for the PHEMA, $PPEGMA_6$ and $PPEGMA_{10}$ brushes studied here are in good agreement with those that have been reported for chemically crosslinked polyacrylamide[39] or zwitterionic carboxybetaine brushes.[40] The Young's moduli of the unmodified PHEMA and $PPEGMA_6$ brushes did not vary significantly with film thickness. For the $PPEGMA_{10}$ brushes, however, increasing film thickness from 29 to 48 nm resulted in an increase in modulus from 2 MPa to 14 MPa. This may be ascribed to crystallization of the oligo(ethylene glycol) side chains in the thick 48 nm films. Related PPEGMA brushes containing a larger number of ethylene glycol side chain repeat units were found to be amorphous for film thicknesses less than 20 nm, whereas crystallization was observed in thicker brushes.[41,42] For the PHEMA and $PPEGMA_6$ brushes, introduction of the RGD peptide results in a significant increase in the modulus (albeit with a significant increase in the scattering of the data for the $PPEGMA_6$ samples as indicated by the larger error bars). This is tentatively attributed to the negatively charged character of the RGD peptide in PBS buffer, which introduces repulsive interchain interactions. For the $PPEGMA_{10}$ brush in contrast, the introduction of the RGD peptide results in a decrease in the modulus. In this case, we speculate that the introduction of the peptide prevents crystallization of the oligo(ethylene glycol) side chains, resulting in a decrease in the modulus as compared to the unmodified $PPEGMA_{10}$ brush.

INSERT FIGURE 7

CONCLUSIONS

Using a diverse set of samples that covered a range of film thicknesses and grafting densities, this study has attempted to provide insight into the swelling behavior and nanomechanical properties of PHEMA and PPEGMA brushes. The swelling behavior of these brushes was investigated by ellipsometry and neutron reflectivity experiments, which revealed swelling ratios that varied from ~ 1.5 - ~5.0. Decreasing the grafting density and decreasing the film thickness generally results in an increase in the swelling ratio. Modification of the PHEMA and PPEGMA brushes with the RGD peptide resulted in a decrease in the swelling ratio. The neutron reflectivity experiments further revealed that solvated PHEMA and PPEGMA brushes are best described by a two-layer model, consisting of a polymer-rich layer close to the substrate and a second layer that is swollen to a much higher degree at the brush – water interface. The Young's moduli of the polymer brushes were determined by AFM nanoindentation experiments. For the unmodified brushes Young's moduli of 1 - 4 MPa were obtained, except for the thickest $PPEGMA_{10}$ brush, which had an apparent Young's modulus of 14 MPa. While introduction of the RGD peptide into PHEMA and $PPEGMA_6$ brushes resulted in an increase in Young's modulus, the opposite effect was observed for $PPEGMA_{10}$ brushes. The results of these experiments may help to design polymer brush based interfaces with predictable interfacial properties.

ACKNOWLEDGMENTS

This work has been financially supported by the Swiss National Science Foundation (SNF) as well as the European Union Seventh Framework Programme (grant agreement n° NMP4-LA-2009-229289 NanoII) (H.-A. K.). Ellipsometry measurements were conducted at the ORNL Centre for Nanophase Materials Sciences, which is a DOE Office of Science User Facility. Neutron reflectivity measurements were carried out at the ORNL Spallation Neutron Source.

ORNL is managed by UT-Battelle, LLC, for the US Department of Energy (DOE) under contract no. DE-AC05-00OR22725. S. M. K. acknowledges support from the National Science Foundation (Award # 1512221). The authors are grateful to Dr. Thomas Geue (PSI, Villigen, Switzerland) for his help with the neutron reflectivity experiments on the RGD modified polymer brushes.

Supporting Information. Cauchy parameters and refractive index profile, AFM data, ellipsometric data, XPS data, NR profiles. This material is available free of charge via the Internet at http://pubs.acs.org

REFERENCES

(1) Stevens, M. M.; George, J. H. Exploring and Engineering the Cell Surface Interface. *Science* **2005**, *310*, 1135-1138.

(2) Discher, D. E.; Janmey, P.; Wang, Y. L. Tissue Cells Feel and Respond to the Stiffness of Their Substrate. *Science* **2005**, *310*, 1139-1143.

(3) Wilson, C. J.; Clegg, R. E.; Leavesley, D. I.; Pearcy, M. J. Mediation of Biomaterial–Cell Interactions by Adsorbed Proteins: A Review. *Tissue Eng*. **2005**, *11*, 1-18.

(4) Shin, H.; Jo, S.; Mikos, A. G. Biomimetic materials for tissue engineering. *Biomaterials* **2003**, *24*, 4353-4364.

(5) Raynor, J. E.; Capadona, J. R.; Collard, D. M.; Petrie, T. A.; Garcia, A. J. Polymer brushes and self-assembled monolayers: Versatile platforms to control cell adhesion to biomaterials (Review). *Biointerphases* **2009**, *4*, FA3-FA16.

(6) Moroni, L.; Gunnewiek, M. K.; Benetti, E. M. Polymer brush coatings regulating cell behavior: Passive interfaces turn into active. *Acta Biomater*. **2014**, *10*, 2367-2378.

(7) Barbey, R.; Lavanant, L.; Paripovic, D.; Schüwer, N.; Sugnaux, C.; Tugulu, S.; Klok, H.-A. Polymer Brushes via Surface-Initiated Controlled Radical Polymerization: Synthesis, Characterization, Properties, and Applications. *Chem. Rev.* **2009**, *109*, 5437-5527.

(8) Ayres, N. Polymer brushes: Applications in biomaterials and nanotechnology. *Polym. Chem.* **2010**, *1*, 769-777.

(9) Zhu, Y..; Gao, C.; Guan, J.; Shen, J. Engineering porous polyurethane scaffolds by photografting polymerization of methacrylic acid for improved endothelial cell compatibility. *J. Biomed. Mater. Res., Part A* **2003**, *67A*, 1367-1373.

(10) Harris, B. P.; Kutty, J. K.; Fritz, E. W.; Webb, C. K.; Burg, K. J..; Metters, A. T. Photopatterned polymer brushes promoting cell adhesion gradients. *Langmuir* **2006**, *22*, 4467-4471.

(11) Navarro, M.; Benetti, E. M.; Zapotoczny, S.; Planell, J. A.; Vancso, G. J. Buried, covalently attached RGD peptide motifs in poly(methacrylic acid) brush layers: the effect of brush structure on cell adhesion. *Langmuir* **2008**, *24* , 10996-11002.

(12) Zhang, Z.; Chen, S.; Jiang, S. Dual-Functional Biomimetic Materials: Nonfouling Poly(carboxybetaine) with Active Functional Groups for Protein Immobilization. *Biomacromolecules* **2006**, *7*, 3311-3315.

(13) Hucknall, A.; Rangarajan, S.; Chilkoti, A. In Pursuit of Zero: Polymer Brushes that Resist the Adsorption of Proteins. *Adv. Mater.* **2009**, *21*, 2441-2446.

(14) Tugulu, S.; Silacci, P.; Stergiopulos, N.; Klok, H.-A. RGD—Functionalized polymer brushes as substrates for the integrin specific adhesion of human umbilical vein endothelial cells. *Biomaterials* **2007**, *28*, 2536-2546.

(15) Desseaux, S. ; Klok, H.-A. Temperature-Controlled Masking/Unmasking of Cell-Adhesive Cues with Poly(ethylene glycol) Methacrylate Based Brushes. *Biomacromolecules* **2014**, *15*, 3859-3865.

(16) Desseaux, S.; Klok, H.-A. Fibroblast adhesion on ECM-derived peptide modified poly(2-hydroxyethyl methacrylate) brushes: Ligand co-presentation and 3D-localization. *Biomaterials* **2015**, *44*, 24-35.

(17) Rahane, S. B.; Floyd, J. A.; Metters, A. T.; Kilbey, S. M. Swelling Behavior of Multiresponsive Poly(methacrylic acid)-block-poly(N-isopropylacrylamide) Brushes Synthesized Using Surface-Initiated Photoiniferter-Mediated Photopolymerization. *Adv. Funct. Mater.* **2008**, *18*, 1232-1240.

(18) Deodhar, C.; Soto-Cantu, E.; Uhrig, D.; Bonessen, P.; Lokitz, B. S.; Ankner, J. F.; Kilbey, S. M. II. Hydration in Weak Polyelectrolyte Brushes. *ACS Macro. Lett.* **2013**, *2*, 398-402.

(19) Tranchida, D.; Sperotto, E.; Staedler, T.; Jiang, X.; Schönherr, H. Nanomechanical Properties of Oligo(ethylene glycol methacrylate) Polymer Brush-Based Biointerfaces. *Adv. Eng. Mater.* **2011**, *13*, B369-B367.

(20) Feng, W.; Nieh, M.-P.; Zhu, S.; Harroun, T. A.; Katsaras, J.; Brash, J. L. Characterization of protein resistant, grafted methacrylate polymer layers bearing oligo (ethylene glycol) and phosphorylcholine side chains by neutron reflectometry. *Biointerphases* **2007**, *2*, 34-43.

(21) Fu, L.; Chen, X.; He, J.; Xiong, C.; Ma, H. Study Viscoelasticity of Ultrathin Poly(oligo(ethylene glycol) methacrylate) Brushes by a Quartz Crystal Microbalance with Dissipation. *Langmuir* **2008**, *24* , 6100-6106.

(22) Bao, Z.; Bruening, M. L.; Baker, G. L. Control of the Density of Polymer Brushes Prepared by Surface-Initiated Atom Transfer Radical Polymerization. *Macromolecules* **2006**, *39*, 5251-5258.

(23) Hersel, U.; Dahmen, C.; Kessler, H. RGD modified polymers: biomaterials for stimulated cell adhesion and beyond. *Biomaterials* **2003**, *24*, 4385-4415.

(24) Schüwer, N.; Klok, H.-A. A Potassium-Selective Quartz Crystal Microbalance Sensor Based on Crown-Ether Functionalized Polymer Brushes *Adv. Mater.* **2010**, *22*, 3251-3255.

(25) Schüwer, N.; Geue, T.; Hinestrosa, J. P.; Klok, H.-A. Neutron Reflectivity Study on the Postpolymerization Modification of Poly(2-hydroxyethyl methacrylate) Brushes. *Macromolecules* **2011**, *44*, 6868-6874.

(26) Spaeth, K.; Kraus, G.; Gauglitz, G. In-situ characterization of thin polymer films for applications in chemical sensing of volatile organic compounds by spectroscopic ellipsometry. *Fresenius J. Anal. Chem.* **1997**, *357*, 292-296.

(27) http://www.ncnr.nist.gov/resources/sldcalc.html

(28) Kilbey, S. M. II; Ankner, J. F. Neutron reflectivity as a tool to understand polyelectrolyte brushes. *Curr. Opin. Colloid Int. Sci.* **2012**, *17*, 83-89.

(29) Butt, H. J.; Jaschke, M. Calculation of thermal noise in atomic I force microscopy. *Nanotechnology* **1995**, *6*, 1-7.

(30) Tugulu, S.; Harms, M.; Fricke, M.; Volkmer, D.; Klok, H.-A. Polymer brushes as ionotropic matrices for the directed fabrication of microstructured calcite thin films. *Angew. Chem., Int. Ed.* **2006**, *45*, 7458-7461.

(31) Voitchovsky, K.; Contera, S. A.; Kamihira, M.; Watts, A.; Ryan, J. F. Differential Stiffness and Lipid Mobility in the Leaflets of Purple Membranes. *Biophys. J.* **2006**, *90*, 2075-2085.

(32) Sugnaux, C.; Lavanant, L.; Klok, H.-A. Aqueous Fabrication of pH-Gated, Polymer-Brush-Modified Alumina Hybrid Membranes. *Langmuir* **2013**, *29*, 7325-7333.

(33) Tugulu, S.; Arnold, A.; Sielaff, I.; Johnsson, K.; Klok, H.-A. Protein-Functionalized Polymer Brushes. *Biomacromolecules* **2005**, *6*, 1602-1607.

(34) Jiang, H.; Xu, F.-J. Biomolecule-functionalized polymer brushes. *Chem. Soc. Rev.* **2013**, *42*, 3394-3426.

(35) Tugulu, S.; Klok, H.-A. Stability and nonfouling properties of poly(poly(ethylene glycol) methacrylate) brushes under cell culture conditions. *Biomacromolecules* **2008**, *9*, 906-912.

(36) Xu, L.-C.; Siedlecki, C. A. Effects of surface wettability and contact time on protein adhesion to biomaterial surfaces. *Biomaterials* **2007**, *28*, 3273-3283.

(37) Jia, H.; Wildes, A.; Titmuss, S. Structure of pH-Responsive Polymer Brushes Grown at the Gold-Water Interface: Dependence on Grafting Density and Temperature. *Macromolecules* **2012**, *45*, 305-312.

(38) Malham, I. B.; Bureau, L. Density Effects on Collapse, Compression, and Adhesion of Thermoresponsive Polymer Brushes. *Langmuir* **2010**, *26*, 4762-4768.

(39) Lilge, I.; Schönherr, H. Covalently cross-linked poly(acrylamide) brushes on gold with tunable mechanical properties via surface-initiated atom transfer radical polymerization. *Eur. Polym. J.* **2013**, *49*, 1943-1951.

(40) Carr, L. R.; Xue, H.; Jiang, S. Functionalizable and nonfouling zwitterionic carboxybetaine hydrogels with a carboxybetaine dimethacrylate crosslinker. *Biomaterials* **2011**, *32*, 961-968.

(41) Zheng, Y.; Bruening, M. L.; Baker, G. L. Crystallization of Polymer Brushes with Poly(ethylene oxide) Side Chains. *Macromolecules* **2007**, *40*, 8212-8219.

(42) Zheng, Y.; Bruening, M. L.; Baker, G. L. Crystallization kinetics of polymer brushes with poly(ethylene oxide) side chains. *J. Polym. Sci., Part B. Polym. Phys.* **2010**, *48*, 1955-1959.

Table 1. Dry film thickness, root mean square (RMS) roughness, water contact angle (WCA) as well as swelling ratio (d_{PBS}/d_{dry}) in PBS of PHEMA, $PPEGMA_6$ and $PPEGMA_{10}$ brushes before and after post-polymerization modification with the GGGRGDS peptide (σ = 100 %). Film thicknesses and RMS values were determined by AFM on micropatterned samples.

	Before post-polymerization modification with RGD				After post-polymerization modification with RGD			
	Thickness in air (nm)	**Roughness in air (nm)**	**WCA(°)**	**Swelling ratio in PBS**	**Thickness in air (nm)**	**Roughness in air (nm)**	**WCA(°)**	**Swelling ratio in PBS**
PHEMA	52 ± 2	0.7	43 ± 2	1.5 ± 0.1	133 ± 2	1.2	46	1.2 ± 0.1
$PPEGMA_6$	50 ± 3	1.0	46 ± 1	1.9 ± 0.1	103 ± 1	1.1	48	0.9 ± 0.1
$PPEGMA_{10}$	48 ± 5	0.6	47 ± 3	1.5 ± 0.2	64 ± 1	1.1	48	1.3 ± 0.1

Table 2. Neutron reflectivity fitting results obtained on densely grafted (σ = 100 %) PHEMA, $PPEGMA_6$ and $PPEGMA_{10}$ brushes (polymerization time = 240 min), both dry as well as D_2O swollen conditions.

Sample	**Condition**	**SLD** ($\times 10^{-6}$ Å^{-2})	**Thickness** (nm)	**Roughness** (nm)	χ^2	d_{D2O}/d_{dry} [(a)] (-)	ϕ [(a)]
PHEMA	Dry	0.99	91.7	4.0	10.2		
	D_2O Layer 1	1.52	52.0	52.0	13.8	1.598	0.643
	D_2O Layer 2	3.71	94.5	7.9			
$PPEGMA_6$	Dry	0.77	76.1	6.1	9.5		
	D_2O Layer 1	1.47	70.5	70.5	10.0	1.862	0.664
	D_2O Layer 2	3.94	71.2	10.3			
$PPEGMA_{10}$	Dry	0.73	76.2	4.8	8.6		
	D_2O Layer 1	1.33	54.3	54.3	8.5	1.842	0.625
	D_2O Layer 2	3.62	85.9	13.2			

[(a)] Overall swelling ratio and polymer volume fraction of the swollen polymer brush film.

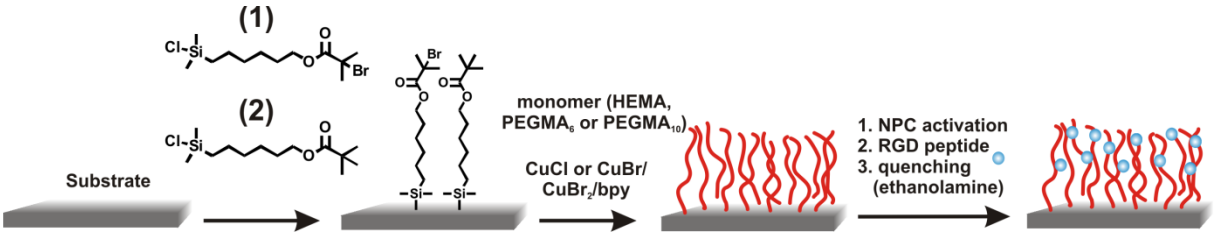
(1)
(2)
Substrate
monomer (HEMA, PEGMA6 or PEGMA10)
CuCl or CuBr/ CuBr2/bpy
1. NPC activation
2. RGD peptide
3. quenching (ethanolamine)

Scheme 1.

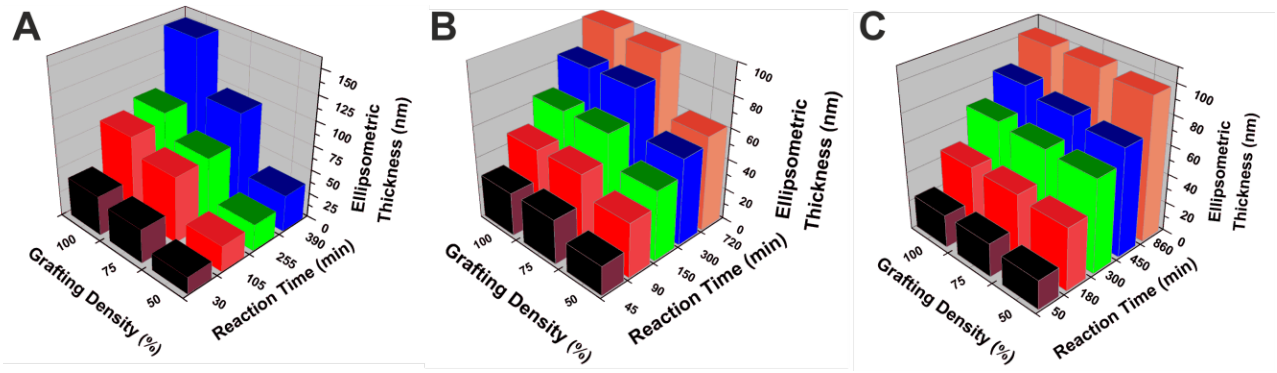

Figure 1. Ellipsometric dry film thickness as a function of polymerization time and grafting density for the surface-initiated atom transfer radical polymerization of: (A) HEMA; (B) $PEGMA_6$; (C) $PEGMA_{10}$. The corresponding 2D plots are included in Supporting Information Figure S4.

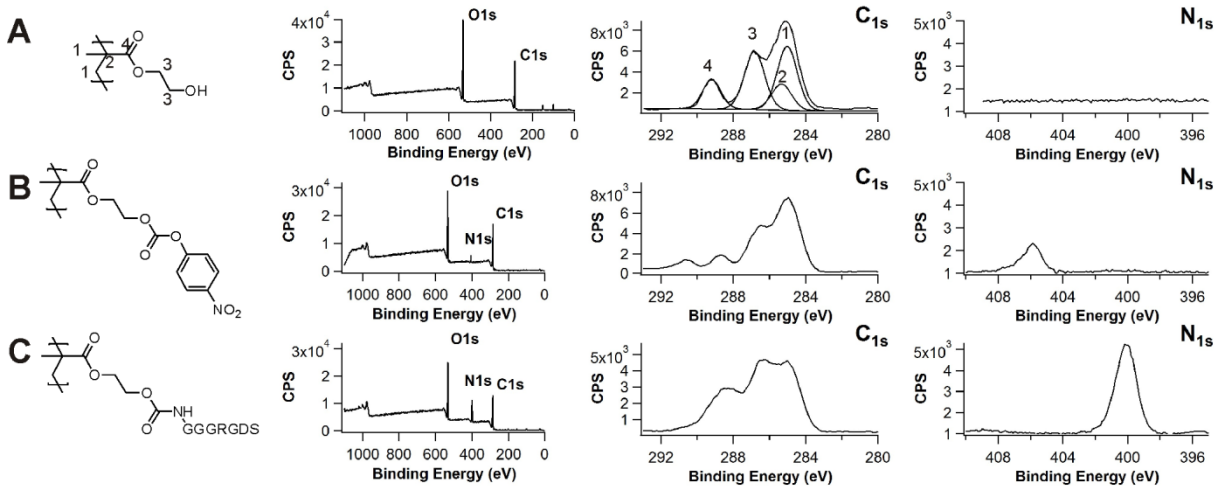

Figure 2. XPS survey spectra as well as C_{1s} and N_{1s} high resolution scans of: (A) a PHEMA brush; (B) a NPC-activated PHEMA brush; (C) a RGD-functionalized PHEMA brush (grafting densities and film thicknesses are indicated in Table 1).

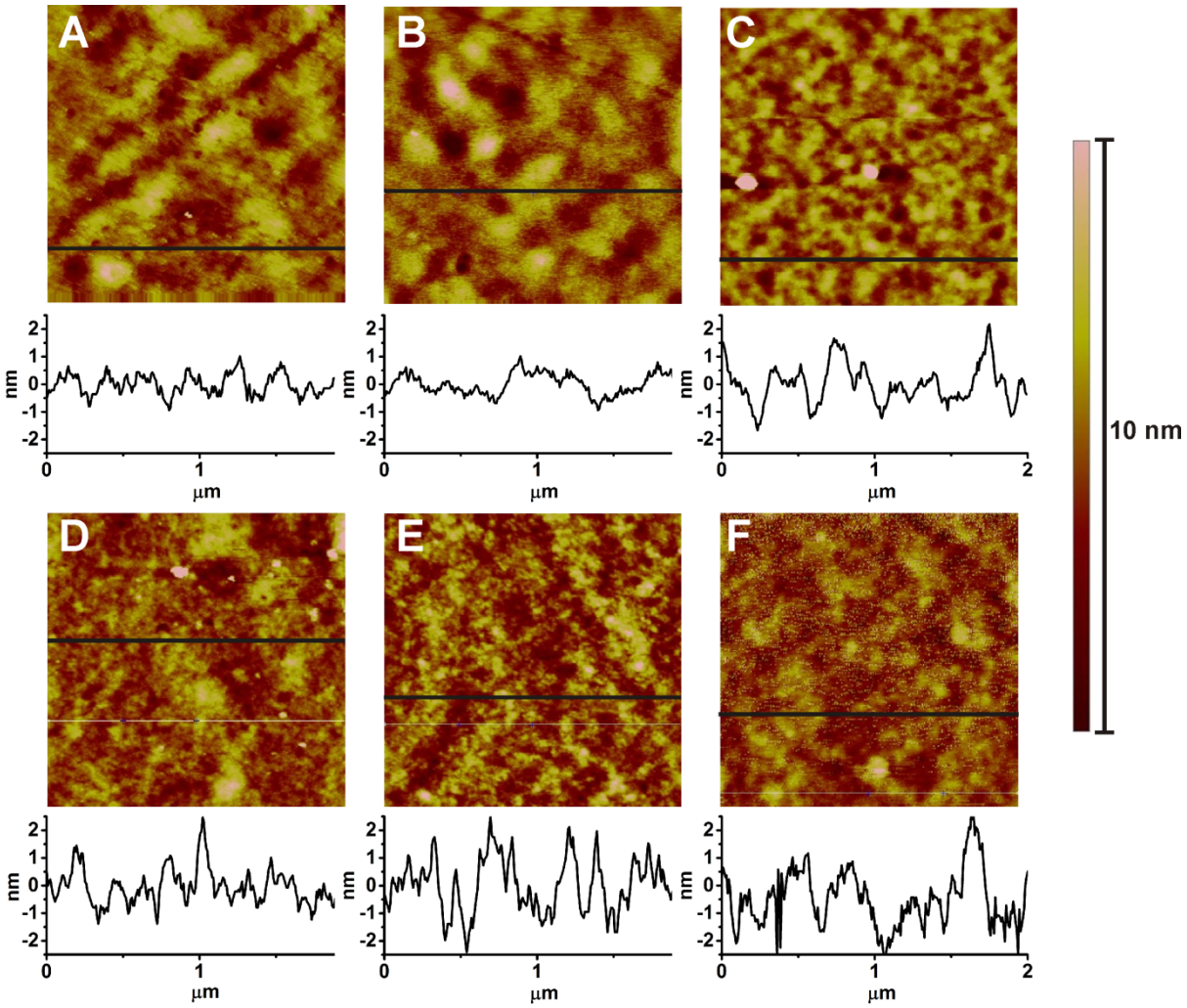

Figure 3. Topography scans recorded in air of: (A) a PHEMA brush; (B) a $PPEGMA_6$ brush; (C) a $PPEGMA_{10}$ brush; (D) a RGD post-modified PHEMA brush; (E) a RGD post-modified $PEGMA_6$ brush and (F) a RGD post-modified $PEGMA_{10}$ brush (scan size: 2 μm x 2 μm) (film thicknesses and grafting densities are reported in Table 1).

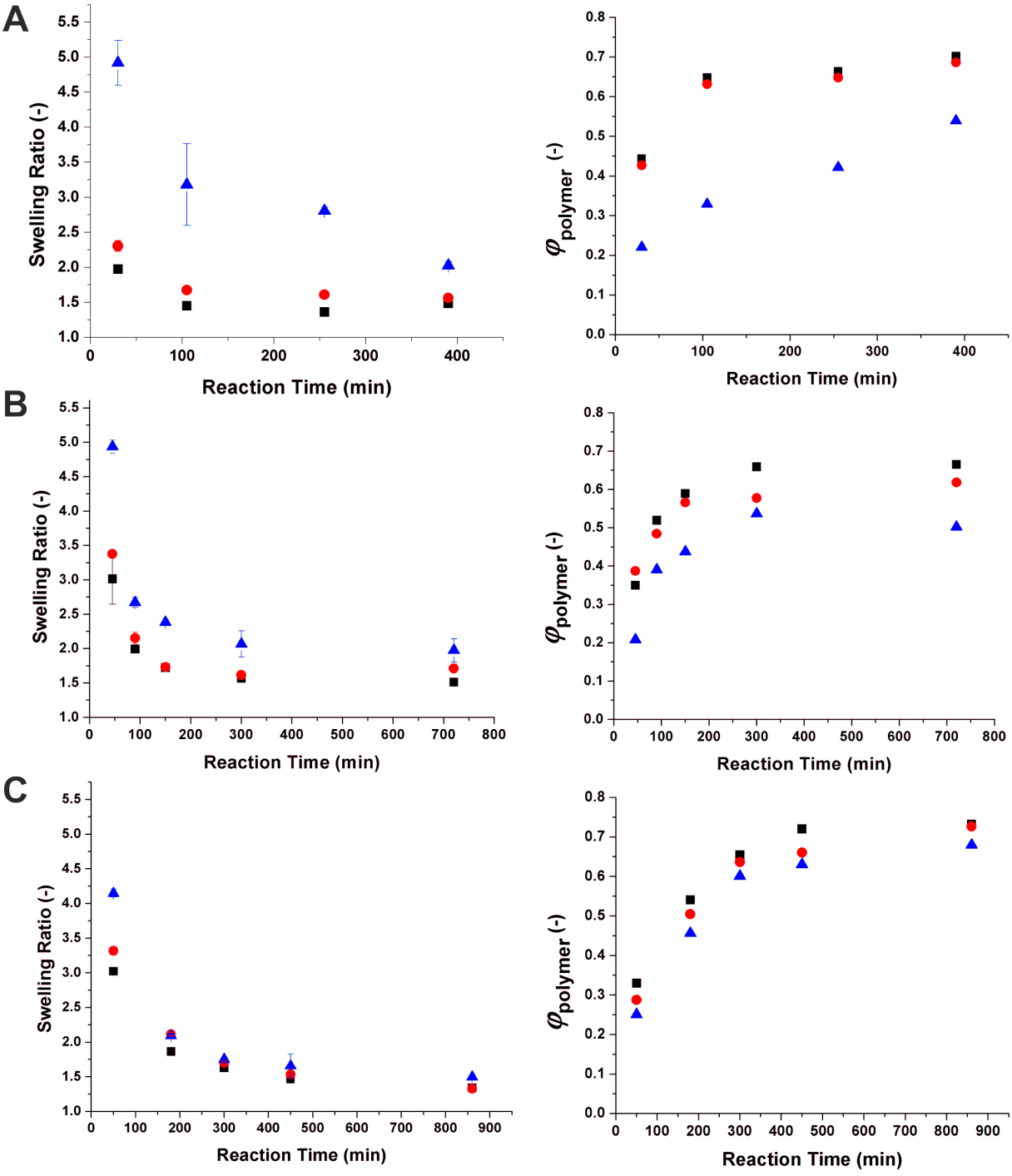

Figure 4. Swelling ratios and polymer fractions from ellipsometry for (A) PHEMA, (B) $PPEGMA_6$ and (C) $PPEGMA_{10}$ brushes at three different grafting densities (■: σ = 100 %, ●: σ = 75 %, ▲: σ = 50 %) as a function of polymerization time. In some instances the error bars are smaller than the data points.

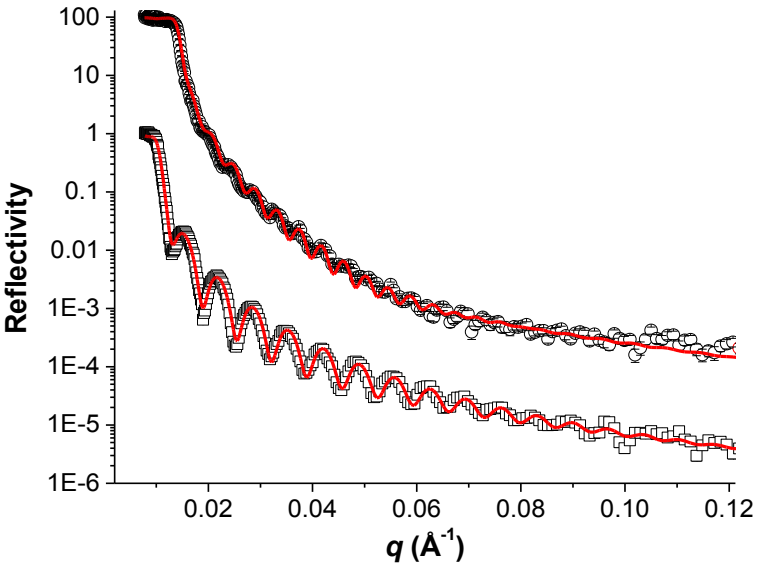

Figure 5. Neutron reflectivity profiles and model fit for a PHEMA brush (d_{dry} = 91.7 ± 4.0 nm; σ = 100 %) in both dry (□) and D_2O swollen (○) conditions. The data set and fit for the swollen brushes are shifted vertically by a factor of 10^2 for clarity.

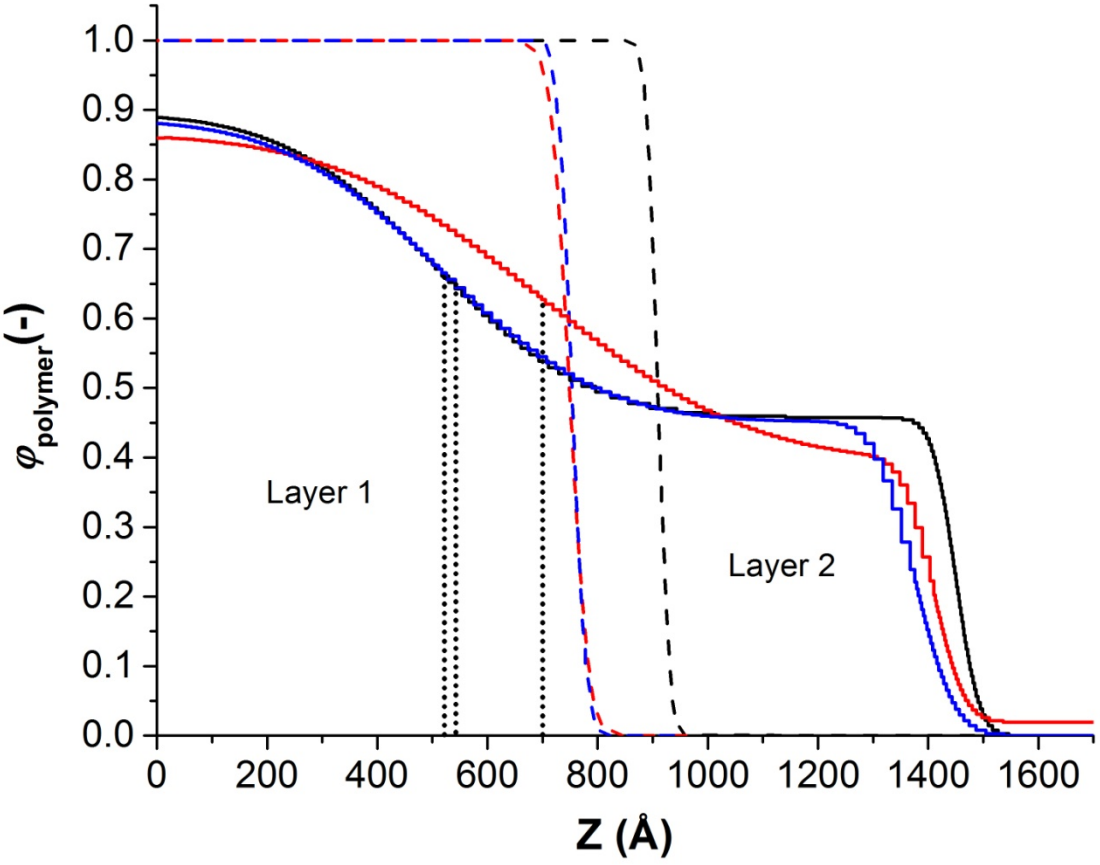

Figure 6. Polymer density profiles from neutron reflectivity for dry (dashed line) and solvated conditions (solid line) for PHEMA brushes (black), $PPEGMA_6$ brushes (red) and $PPEGMA_{10}$ brushes (blue) at σ = 100% (polymerization time = 240 min). Swollen brushes required 2 layers to fit the data, so the vertical dotted lines represent the "interface" between those two layers. (Layer thicknesses and "roughnesses", which describe the transition from one layer to the next, are listed in Table 2).

.

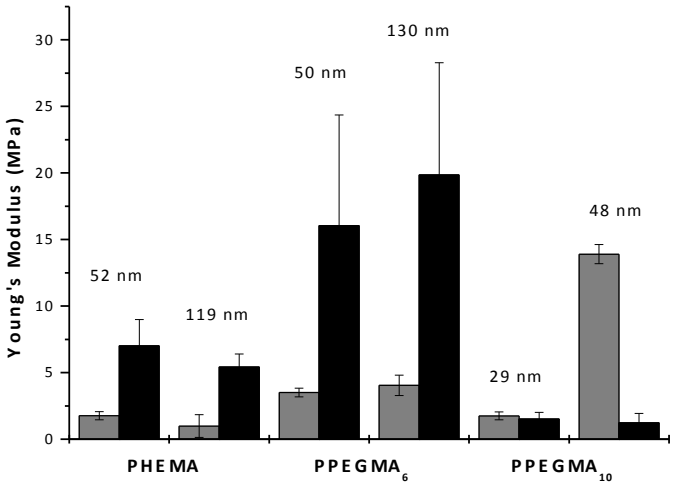

Figure 7. Apparent Young's moduli in PBS of polymer brush samples before (gray) and after post-polymerization modification with the RGD peptide (black). The AFM measured thickness of the dry polymer brush before post-polymerization modification is indicated above each sample.

Table of Contents Graphic